JACC: CARDIOVASCULAR INTERVENTIONS VOL. 3, NO. 9, 2010

ISSN 1936-8798/$36.00
PUBLISHED BY ELSEVIER INC. DOI: 10.1016/j.jcin.2010.05.016

Reparative Effects of Allogeneic Mesenchymal Precursor Cells Delivered Transendocardially in Experimental Nonischemic Cardiomyopathy

Peter J. Psaltis, MD, PhD,*† Angelo Carbone, BSc,* Adam J. Nelson, BMedSc,* Dennis H. Lau, MD,* Troy Jantzen, PhD,§ Jim Manavis, BSc,‡ Kerry Williams, Dip AppSc,* Silviu Itescu, MD, PhD,‖ Prashanthan Sanders, MD, PhD,* Stan Gronthos, PhD,† Andrew C. W. Zannettino, PhD,† Stephen G. Worthley, MD, PhD*

Adelaide and Sydney, Australia; and New York, New York

Objectives This study set out to evaluate the safety and efficacy of allogeneic bone marrow mesenchymal precursor cells (MPC) delivered by multisegmental, transendocardial implantation in the setting of nonischemic cardiomyopathy (NICM).

Background Prospectively isolated MPC have shown capacity to mediate cardiovascular repair in myocardial ischemia. However, their efficacy in NICM remains undetermined.

Methods Mesenchymal precursor cells were prepared from ovine bone marrow by immunoselection using the tissue nonspecific alkaline phosphatase, or STRO-3, monoclonal antibody. Fifteen sheep with anthracycline-induced NICM were assigned to catheter-based, transendocardial injections of allogeneic MPC ($n = 7$) or placebo ($n = 8$), under electromechanical mapping guidance. Follow-up was for 8 weeks, with end points assessed by cardiac magnetic resonance, echocardiography, and histology.

Results Intramyocardial injections were distributed similarly throughout the left ventricle in both groups. Cell transplantation was associated with 1 death late in follow-up, compared with 3 early deaths among placebo animals. Left ventricular end-diastolic size increased in both cohorts, but MPC therapy attenuated end-systolic dilation and stabilized ejection fraction, with a nonsignificant increase (37.3 ± 2.8% before, 39.2 ± 1.4% after) compared with progressive deterioration after placebo (38.8 ± 4.4% before, 32.5 ± 4.9% after, $p < 0.05$). Histological outcomes of cell therapy included less fibrosis burden than in the placebo group and an increased density of karyokinetic cardiomyocytes and myocardial arterioles ($p < 0.05$ for each). These changes occurred in the presence of modest cellular engraftment after transplantation.

Conclusions Multisegmental, transendocardial delivery of cell therapy can be achieved effectively in NICM using electromechanical navigation. The pleiotropic properties of immunoselected MPC confer benefit to nonischemic cardiac disease, extending their therapeutic potential beyond the setting of myocardial ischemia. (J Am Coll Cardiol Intv 2010;3:974–83) © 2010 by the American College of Cardiology Foundation

From the *Cardiovascular Research Centre, Royal Adelaide Hospital and Department of Medicine, University of Adelaide, Adelaide, Australia; the †Bone and Cancer Laboratories, Division of Hematology, Institute of Medical and Veterinary Science, Adelaide, Australia; the ‡Hanson Institute Centre for Neurological Diseases, Institute of Medical and Veterinary Science, Adelaide, Australia; §Biosense-Webster, Johnson & Johnson Medical, Sydney, Australia; and ‖Angioblast Systems, Ltd., New York, New York. Dr. Psaltis has received funding from the National Health and Medical Research Council of Australia, National Heart Foundation of Australia, and Royal Adelaide Hospital. Dr. Nelson is a research student at Royal Adelaide Hospital. Dr. Lau has received funding from the National Health and Medical Research Council of Australia and the University of Adelaide and Kidney Health Australia. Dr. Jantzen is an employee of Biosense-Webster, Australia and Johnson & Johnson Medical. Dr. Sanders has served on the advisory board and received lecture fees and research funding from Medtronic, Inc., St. Jude Medical, Bard Electrophysiology, Biosense-Webster, Sanofi-Aventis, and Merck Sharpe and Dohme. Professor Itescu is the Founder/Chief Scientist of Angioblast Systems Inc. All other authors report that they have no relationships to disclose.

Manuscript received March 25, 2010; revised manuscript received May 3, 2010, accepted May 15, 2010.

Nonischemic cardiomyopathy (NICM) contributes to approximately one-third of clinical cardiac failure and comprises numerous etiologies, some of which are especially refractory to current management options (1). Despite the interest in cell-based therapies for ischemic heart disease (2), there has been a paucity of studies investigating their utility in nonischemic disease. Recent reports have described the intracoronary administration of autologous, unselected bone marrow (BM) cells to patients with NICM (3,4). However, the safety and efficacy of other cell types and methods of delivery remain understudied, beyond the setting of small animal research (5–7).

Bone marrow mesenchymal stromal/stem cells (MSC) are multipotent cells that are notable for their ease of isolation, proclivity for expansion, and unique immunoregulatory properties, which may enable their allogeneic use for tissue repair (8). In pre-clinical and clinical studies of myocardial infarction and chronic ischemia, these cells have demonstrated the capacity to improve cardiac perfusion and augment contractile function (9–12). These studies have predominantly used BM MSC prepared by simple plastic adherence-isolation (13). This nonselective technique has several limitations that may restrict the stemlike characteristics of conventional MSC preparations (14). Prospective isolation is an alternative strategy that aims to selectively enrich for immature mesenchymal precursor cells (MPC) at high purity, based on their expression of cell surface antigens that can be targeted by specific monoclonal antibodies (mAb) (e.g., stromal precursor antigen-1 [STRO-1], tissue nonspecific alkaline phosphatase [STRO-3]) (15,16). Previously, we have shown that selective preparation of MPC enhances their cardiovascular trophic effects in vitro (14), and that these cells impart provasculogenic and antifibrotic effects to the myocardium after experimental myocardial infarction (17,18).

In the current study, we hypothesized that the pleiotropic characteristics of MPC may also confer reparative benefit to nonischemic heart disease. We used an ovine model of anthracycline-induced NICM (19) to investigate the safety and efficacy of allogeneic BM STRO-3–selected MPC, delivered by multisegmental, transendocardial injections under electromechanical guidance.

Methods

For an expanded description, see the Online Appendix.

Ovine model of NICM. Animal experiments conformed to the "Guide for the Care and Use of Laboratory Animals" published by the U.S. National Institutes of Health (NIH Publication No. 85-23, revised 1985) and were approved by the institutional Animal Ethics Committee.

The study protocol is summarized in Online Figure 1. Fifteen Merino wether sheep (weight 45 to 55 kg) underwent baseline cardiac evaluation before receiving serial intracoronary doses of the anthracycline agent, doxorubicin, to induce NICM, as previously described (19). In brief, doxorubicin (1 mg/kg) was infused into the left-sided coronary arteries under fluoroscopic guidance, with a 5-F Amplatz diagnostic catheter (ALI, Cordis Corporation, Miami Lakes, Florida). Doses were repeated every 2 weeks until animals showed echocardiographic evidence of left ventricular (LV) systolic dysfunction (fractional shortening <25%). Ten weeks after the first doxorubicin exposure, cardiac assessment was repeated with cardiac magnetic resonance, transthoracic echocardiography, and left and right heart catheterization. Animals were then randomized to transendocardial injections of allogeneic MPC (n = 7) or placebo (n = 8).

Cell preparation. Mesenchymal precursor cells were prepared by STRO-3–based, magnetic-activated, Dynal bead selection from BM mononuclear cells (MNC) of male Rambouillet strain sheep (16,18). These cells were characterized in vitro for clonogenicity, surface immunophenotype, and multilineage differentiation potential.

Passage 4 MPC were used for transplantation and were transduced with retroviral particles encoding green fluorescence protein (GFP) to investigate for cellular engraftment. Cryopreservation was performed in a mixture containing ProFreeze NAO Freezing Medium (Lonza Bio Whittaker, Walkersville, Maryland), which was also used as placebo. Immediately prior to injection, frozen preparations were thawed at 37°C and cell viability and number were assessed by trypan blue exclusion.

Abbreviations and Acronyms

BM = bone marrow
GFP = green fluorescence protein
LV = left ventricular
mAb = monoclonal antibodies
MNC = mononuclear cells
MPC = mesenchymal precursor cells
MSC = mesenchymal stromal/stem cells
NICM = nonischemic cardiomyopathy
STRO-3 = tissue nonspecific alkaline phosphatase monoclonal antibody

Intramyocardial injections. Percutaneous LV electromechanical mapping (NOGA XP Cardiac Navigation System, Biologics Delivery Systems Group, Cordis Corporation, Diamond Bar, California) was performed just before cell/placebo injections, using standard methodology (20). Three-dimensional map reconstructions of unipolar voltage amplitude and linear local shortening ratio were used to delineate regional abnormalities of myocardial electrical viability and/or mechanical function.

Transendocardial injections were performed with 8-F MyoStar catheters (Biologics Delivery Systems) (Online Fig. 2). Each animal received 20 injections (0.2 ml/injection), distributed throughout the left ventricle, target-

ing areas of reduced linear local shortening ratio (<11.5%) and/or unipolar voltage amplitude (<7.5 mV) (Figs. 1A and 1B). These threshold values had been determined in a previous validation study (21). The apex and posterior wall were injected less frequently to avoid cardiac perforation and due to difficulty in establishing catheter tip stability near the papillary muscles. Injections were administered at a rate of 0.1 ml/15 s and standard criteria were used to ensure satisfactory intramyocardial delivery (20).

Animals were followed for 8 weeks after transendocardial intervention, at which time they were restudied with cardiac magnetic resonance, transthoracic echocardiography, and hemodynamic measurements before euthanasia (sodium pentobarbital 120 mg/kg).

Histopathology. In addition to study animals, 4 weight-matched, healthy sheep were used to provide reference to "normal" histology. Hearts were excised, weighed, perfusion-fixed (4% paraformaldehyde), and immersed in 10% buffered formalin. The LV was cut transversely at 1-cm intervals. Slices from the basal, mid, and distal levels were each divided into 4 segments (anterior, septal, posterior, and lateral), which along with the apex provided 13 segments for analysis. After paraffin embedding, contiguous 5-μm sections were taken from each segment for staining with hematoxylin and eosin, Masson's trichrome, and immunohistochemistry.

Masson's trichrome slides were analyzed with semiautomated analySIS Pro software (Olympus Soft Imaging Solutions GmbH, Muenster, Germany) to determine the percentage area of myocardium occupied by fibrosis (blue color) for each segment and for the LV overall.

The effects of MPC transplantation on cardiomyocyte karyokinesis and myocardial vascularity were evaluated by manual counting of $Ki67^{+}$/$desmin^{+}$ cells and alpha-smooth muscle actin-positive vascular structures, respectively. Twelve fields of view (4 subendocardial, 4 midmural, 4 subepicardial) were examined at ×20 magnification for each myocardial segment. Results were expressed as the average count per field of view for each of the animal groups.

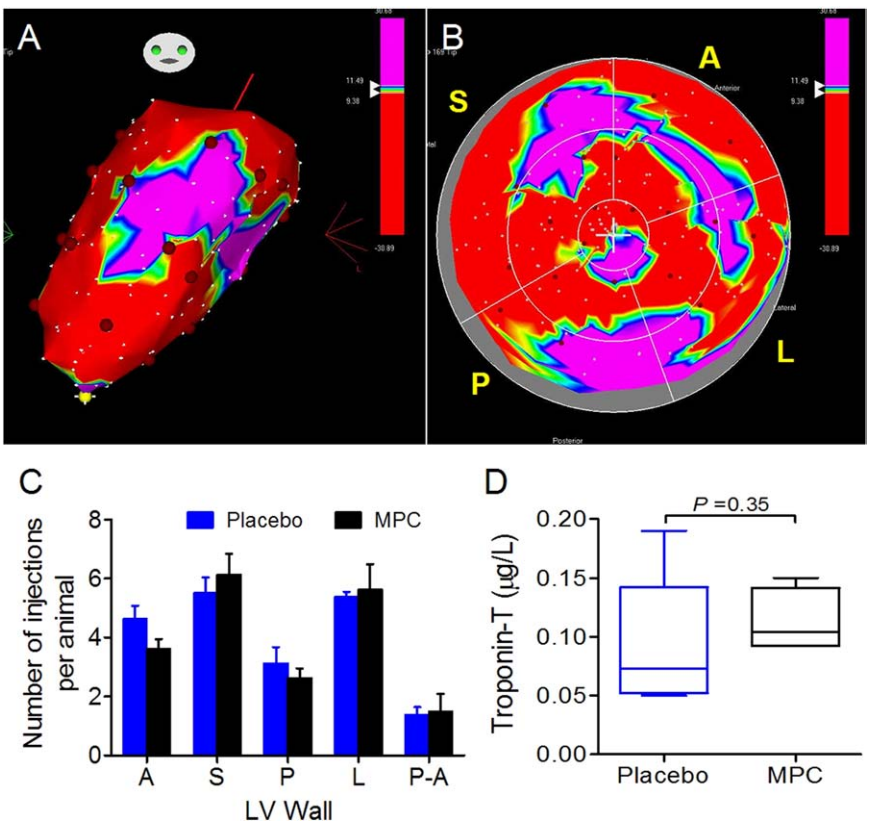

Figure 1. Intramyocardial Injections

(A, B) Representative anteroposterior **(A)** and "bull's-eye" **(B)** projections of a linear local shortening map display the multisegmental distribution of injection sites **(brown circles)** (linear local shortening: **purple:** >11.5%, **red:** <9.3%). **(C)** There was no significant difference in the segmental location of injection sites between the 2 treatment groups. Results shown are mean ± SEM. **(D)** Intramyocardial delivery was followed by minor elevations of serum troponin-T in both cohorts, without significant intergroup difference. **Whisker bars** show median value **(horizontal line)**, with 25th to 75th interquartile range **(box)** and minimum and maximum range **(bars)**. A = anterior; L = lateral; LV = left ventricular; MPC = mesenchymal precursor cells; P = posterior; P-A = periapical; S = septal.

Statistical analysis. All analyses were performed blind to study group. Normality of data distribution was assessed by Shapiro-Wilk test where indicated and continuous variables reported as mean ± SEM. Intragroup comparisons at different time points were performed by paired Student *t* test or repeated measures analysis of variance. Intergroup comparisons involved unpaired Student *t* test, 2-way or 1-way analysis of variance, with Tukey post-hoc test, as appropriate. Statistical significance was established at 2-tailed $p < 0.05$.

Results

Immunopreparation of MPC. Enrichment for STRO-3 increased recovery of colony forming units-fibroblast from Rambouillet BM MNC, by approximately 3-fold compared with unfractionated MNC ($p < 0.05$) (Online Fig. 3A). Mesenchymal precursor cells, prepared by in vitro expansion of STRO-3$^+$ MNC, demonstrated multilineage developmental potential by producing mineral, fat, and cartilage matrix under inductive culture conditions (Online Fig. 3B) and fulfilled the immunophenotypic criteria of MSC ($CD29^+/CD44^+/CD166^+/CD45^-/CD14^-/CD31^-$) (Online Fig. 3C).

Pre-injection characteristics of doxorubicin-treated sheep. The 15 sheep (46.5 ± 0.7 kg) that were randomized to placebo or MPC had received a cumulative doxorubicin dose of 3.7 ± 0.1 mg/kg (range 3 to 4 mg/kg). At the time of NOGA XP-guided intervention, mean ejection fraction had decreased from 45.5 ± 1.5% to 37.1 ± 1.8% ($p < 0.01$). Both groups were similar for hemodynamic parameters, LV chamber size, and systolic function (Table 1).

Intramyocardial cell transplantation. Total injection time was 61 ± 3 min/case. Average MPC dose was 109 ± 5 × 10^6 cells per animal or 5.5 ± 0.2 × 10^6 cells per injection, with stable cell viability (88.4 ± 1.8%) maintained throughout the duration of injection procedures. The distribution of injection sites was similar in both groups (Fig. 1C). Two placebo surgeries were complicated by supraventricular tachycardia that resolved quickly with temporary removal of the injection catheter. All cases were associated with small increases in 24-h troponin-T titers (Fig. 1D). Significant changes in systemic inflammatory markers (e.g., white cell count, C-reactive protein) were not observed after treatment.

Survival. One animal receiving MPC was euthanized at 4 weeks to allow for histological detection of GFP-labeling and cell engraftment. In the remaining animals, there were 3 pre-mature deaths in the placebo group (3 of 8) and 1 in the MPC group (1 of 6) ($p = 0.58$ by Fisher exact test). The placebo deaths occurred between weeks 2 and 3 of follow-up from progressive cardiac failure (n = 1) and sudden cardiac arrest (n = 2). The animal that died after cell therapy developed polymorphic ventricular tachycardia during anesthetic induction for follow-up cardiac magnetic resonance.

Cardiac remodeling and function. In animals that were followed for 8 weeks after placebo intervention, there was a

Table 1. Pre-Injection Characteristics of Study Animals

	Placebo (n = 8)		MPC (n = 7)	
	Baseline	Pre-Injection	Baseline	Pre-Injection
Doxorubicin dose, mg/kg		3.7 ± 0.2		3.6 ± 0.2
Body weight, kg	46.1 ± 0.8	48.6 ± 1.2	47.0 ± 1.2	49.5 ± 0.7
Hemodynamics				
Heart rate, beats/min	94.3 ± 2.6	94.1 ± 3.6	92.3 ± 4.7	98.2 ± 5.7
Mean arterial pressure, mm Hg	76.9 ± 1.6	70.9 ± 3.7	79.6 ± 2.5	72.0 ± 2.6*
LV end-diastolic pressure, mm Hg	10.0 ± 0.5	13.4 ± 1.3*	11.3 ± 0.7	14.9 ± 1.2†
PCWP, mm Hg	5.9 ± 0.7	8.6 ± 0.6†	5.8 ± 0.6	8.7 ± 0.5‡
Cardiac index, l/min/m^2	3.0 ± 0.1	3.0 ± 0.2	3.0 ± 0.2	2.9 ± 0.2
Cardiac magnetic resonance				
LV EDV, ml	78.3 ± 6.8	82.3 ± 3.6	77.0 ± 3.8	80.0 ± 3.8
LV ESV, ml	44.5 ± 4.9	51.0 ± 3.8	42.9 ± 4.5	50.0 ± 2.4
LV EF, %	44.9 ± 1.8	36.9 ± 2.9*	46.2 ± 3.0	37.4 ± 2.1*
Echocardiography				
LV EDD, mm	42.3 ± 0.9	43.6 ± 1.1	40.4 ± 1.1	42.7 ± 1.2
LV ESD, mm	28.2 ± 1.1	33.0 ± 1.4*	28.0 ± 1.1	33.2 ± 1.3*
LV FS, %	33.6 ± 1.4	24.0 ± 1.4‡	31.0 ± 1.1	22.5 ± 1.1‡

Results are shown as mean ± SEM. There were no significant intergroup differences between placebo and MPC animals at baseline or pre-injection.
*$p < 0.05$, †$p < 0.01$, ‡$p < 0.001$ for intragroup comparisons between baseline and pre-injection.
EDD = end-diastolic dimension; EDV = end-diastolic volume; EF = ejection fraction; ESD = end-systolic dimension; ESV = end-systolic volume; FS = fractional shortening; LV = left ventricular; MPC = mesenchymal precursor cells; PCWP = pulmonary capillary wedge pressure.

JACC: CARDIOVASCULAR INTERVENTIONS, VOL. 3, NO. 9, 2010
SEPTEMBER 2010:974–83

relative increase in LV end-diastolic volume of 26.0 ± 2.3%, compared with 18.3 ± 7.6% after MPC intervention (n = 5 for each group, p = 0.19 for intergroup comparison) (Fig. 2A). Placebo sheep also developed end-systolic dilation ($p < 0.01$) and further reduction of systolic function, with LV ejection fraction decreasing from 38.8 ± 4.4% to 32.5 ± 4.9% ($p < 0.05$). In contrast, cell therapy attenuated the expansion of end-systolic size (Figs. 2C and 2D) and was accompanied by a nonsignificant increase in ejection fraction (37.3 ± 2.8% to 39.2 ± 1.4%) (Fig. 2E) and improvement in fractional shortening ($p < 0.01$) (Fig. 2F) (Online Fig. 4). Mean arterial pressure and pulmonary capillary wedge pressure also deteriorated after placebo ($p < 0.05$) but remained stable or improved in the MPC cohort over 8-week follow-up (Figs. 3B and 3C).

Intracoronary doxorubicin resulted in slowing of LV activation time, from 21.5 ± 2.4 ms at baseline to 63.7 ± 5.3 ms immediately prior to cell/placebo intervention (n = 15 animals, $p < 0.001$). Electrical activation was further delayed in the 5 animals that survived after placebo intervention ($p < 0.05$), but remained unchanged in the MPC

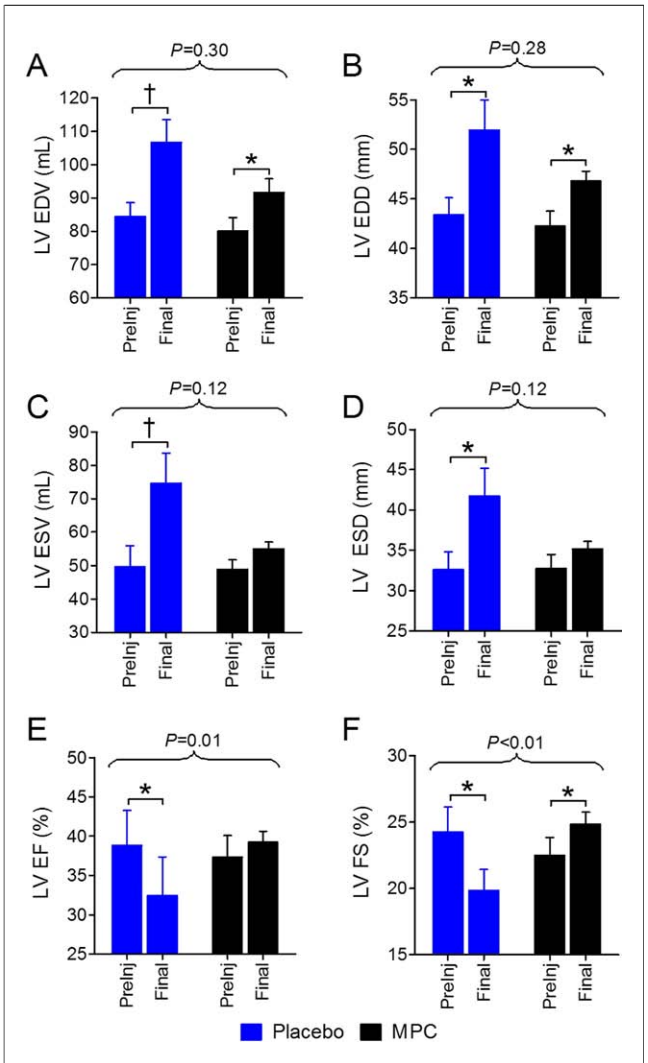

Figure 2. Effect of MPC on LV Size and Function

Graphs show the progress of left ventricular end-diastolic volume, end-diastolic dimension, end-systolic volume, end-systolic dimension, ejection fraction, and fractional shortening for both groups. Data are shown as mean ± SEM. n = 5 surviving animals per group. *$p < 0.05$, †$p < 0.01$ for intragroup comparisons by paired *t* test. Intergroup comparisons performed by 2-way analysis of variance. EDD = end-diastolic dimension; EDV = end-diastolic volume; EF = ejection fraction; ESD = end-systolic dimension; ESV = end-systolic volume; FS = fractional shortening; PreInj = pre-injection; other abbreviations as in Figure 1.

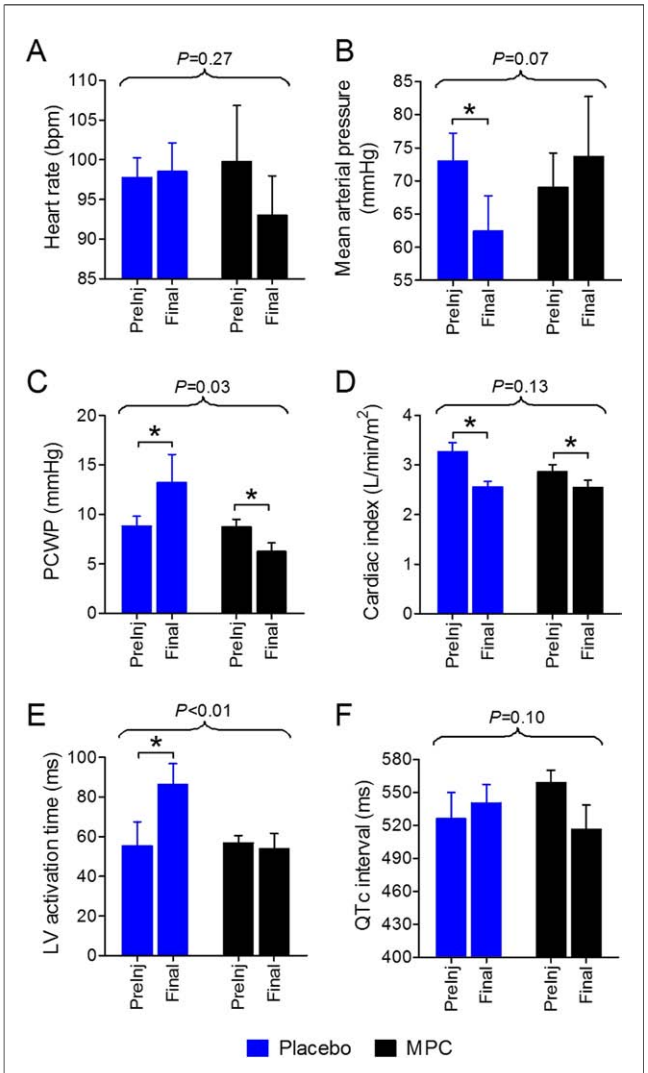

Figure 3. Effect of MPC on Hemodynamic and Electrical Parameters

Graphs display the progress of heart rate **(A)**, mean arterial pressure **(B)**, pulmonary capillary wedge pressure **(C)**, cardiac index **(D)**, total electrical activation time **(E)**, and corrected QT interval **(F)** for both groups. Data are shown as mean ± SEM. n = 5 surviving animals per group. *$p < 0.05$, †$p < 0.01$ for intragroup comparisons by paired *t* test. Intergroup comparisons performed by 2-way analysis of variance. PCWP = pulmonary capillary wedge pressure; QTc = corrected QT interval; other abbreviations as in Figures 1 and 2.

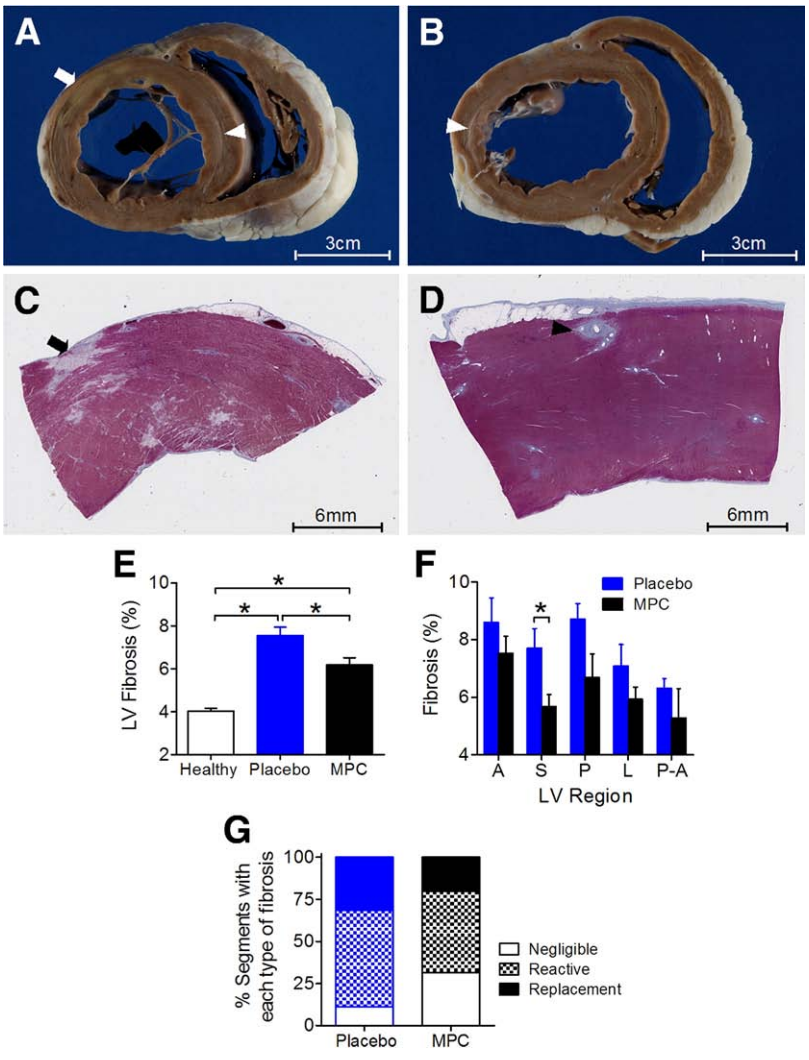

Figure 4. Effect of MPC on Myocardial Fibrosis

Necropsy slices of left ventricle display regions of midmural **(white arrowhead)** and subepicardial **(white arrow)** pallor from the placebo **(A)** and mesenchymal precursor cells (MPC) **(B)** groups. Masson's trichrome sections show foci of replacement fibrosis **(black arrow)** in a placebo-treated heart **(C)** and perivascular fibrosis **(black arrowhead)** after cell therapy **(D)**. Both treatment groups had increased fibrosis burden compared with healthy control hearts, although this was less in the MPC cohort (1-way analysis of variance $p < 0.001$) **(E)**. There were trends toward reduced fibrosis in all myocardial walls of MPC sheep (2-way analysis of variance $p < 0.01$), reaching statistical significance in the septum **(F)**. Sheep that had received cell transplantation had a higher proportion of myocardial segments with negligible fibrosis and fewer segments with either reactive or replacement fibrosis **(G)**. *$p < 0.05$. Abbreviations as in Figures 1 and 2.

group (Fig. 3E). Corrected QT interval was also increased after doxorubicin exposure (474 ± 22 ms at baseline vs. 543 ± 14 ms prior to cell/placebo, n = 15 animals, $p < 0.05$), but showed subsequent improvement in 4 of the 5 animals followed after MPC therapy, an effect not seen in any of the placebo group (Fig. 3F).

Myocardial fibrosis. Total heart weight–to–body weight ratio did not differ significantly between the groups (placebo 6.1 ± 0.2 g/kg, MPC 5.5 ± 0.3 g/kg; p = 0.12). At necropsy, there were multifocal areas of scar and pallor, evident on the epicardial and cut surfaces of the LV, that were more prominent in placebo-treated hearts (Figs. 4A and 4B). No cases of intracardiac tumor formation, ectopic bone, or cartilage were observed in hearts that had received MPC.

Doxorubicin exposure was associated with increased LV fibrosis burden compared with healthy control hearts ($p < 0.05$), comprising both reactive (perivascular or interstitial) and replacement fibrosis, with the latter typically located in subepicardial or midmural myocardium (Figs. 4C and 4D). Importantly, fibrosis was lower after cell transplantation compared with placebo ($p < 0.05$) (Figs. 4E and 4G), with

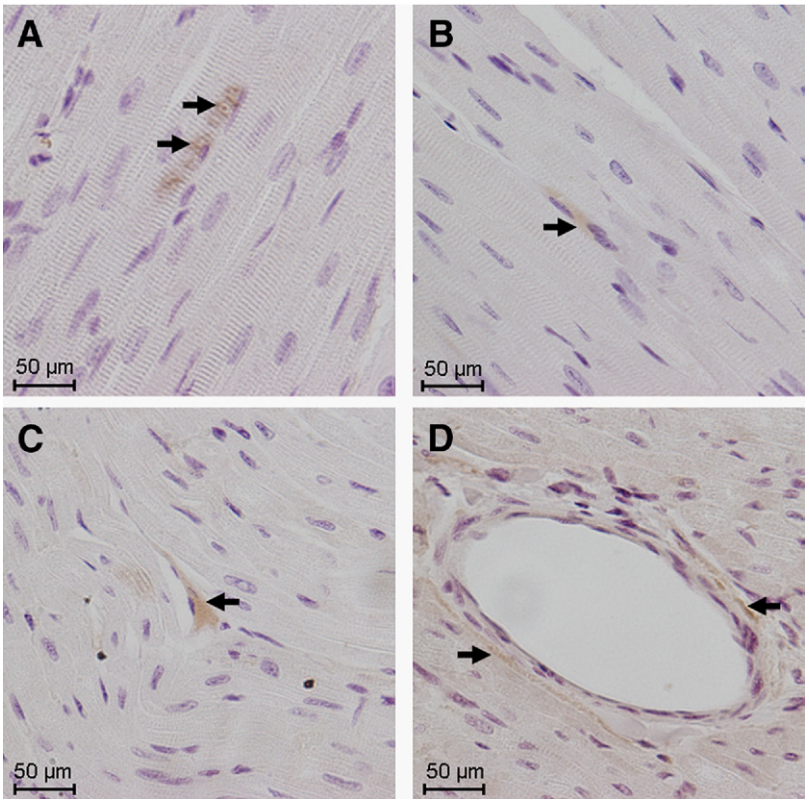

Figure 5. Cell Engraftment

Cells labeled with green fluorescence protein were identified by immunohistochemistry (**brown-stained cells** denoted by **arrows**) and were located sparsely among endogenous cardiomyocytes **(A, B)** and around capillaries **(C)** and larger blood vessels **(D)**.

all myocardial regions showing trends of reduced collagen content in the MPC group, especially the interventricular septum (Fig. 4F).

Cell engraftment. Sparse GFP^+ cells were detected in all LV segments, with even distribution between subendocardial, midmural, and subepicardial layers of the myocardium. These engrafted cells were incorporated among cardiomyocytes (Figs. 5A and 5B) and in perivascular areas, surrounding capillaries, sinusoidal vessels, small and large arterioles, and arteries (Figs. 5C and 5D).

Cardiomyocyte karyokinesis and arteriolar density. $Ki67^+$ cardiac cells were present at low frequency in healthy control animals. Although their average density was elevated in doxorubicin-treated, placebo sheep, they were approximately twice as prevalent following MPC transplantation ($p < 0.05$ vs. placebo) (Fig. 6A) and this differential was observed in all LV walls (Fig. 6B).

Cell therapy was also associated with a 1.5-fold density of alpha-smooth muscle actin-positive blood vessels in the myocardium compared with healthy controls and placebo-treated sheep ($p < 0.05$) (Fig. 6C). In keeping with the multisegmental approach to intramyocardial delivery, this provascular effect was also found to be widespread throughout the LV (Fig. 6D).

Discussion

Despite advances in the management of heart failure, poor prognosis may still accompany NICM (1), justifying evaluation of experimental therapeutic strategies, such as cell transplantation. This pre-clinical study describes for the first time, the strategy of delivering cell therapy by guided, multisegmental, transendocardial injections in NICM. In this context, we have shown pleiotropic reparative benefits from allogeneic, STRO-3–selected BM MPC, consisting of attenuation of cardiac dysfunction, reduction of myocardial fibrosis, and augmentation of cardiac cell cycling and myocardial vascularity.

Immunopreparation of MPC. The vast majority of studies that have previously evaluated BM MSC in cardiovascular disease have focused on ischemic disease models and have used conventionally isolated MSC (8,13). In contrast to plastic adherence isolation, prospective immunoselection uses specific mAb to enrich for immature MPC at higher purity. Although

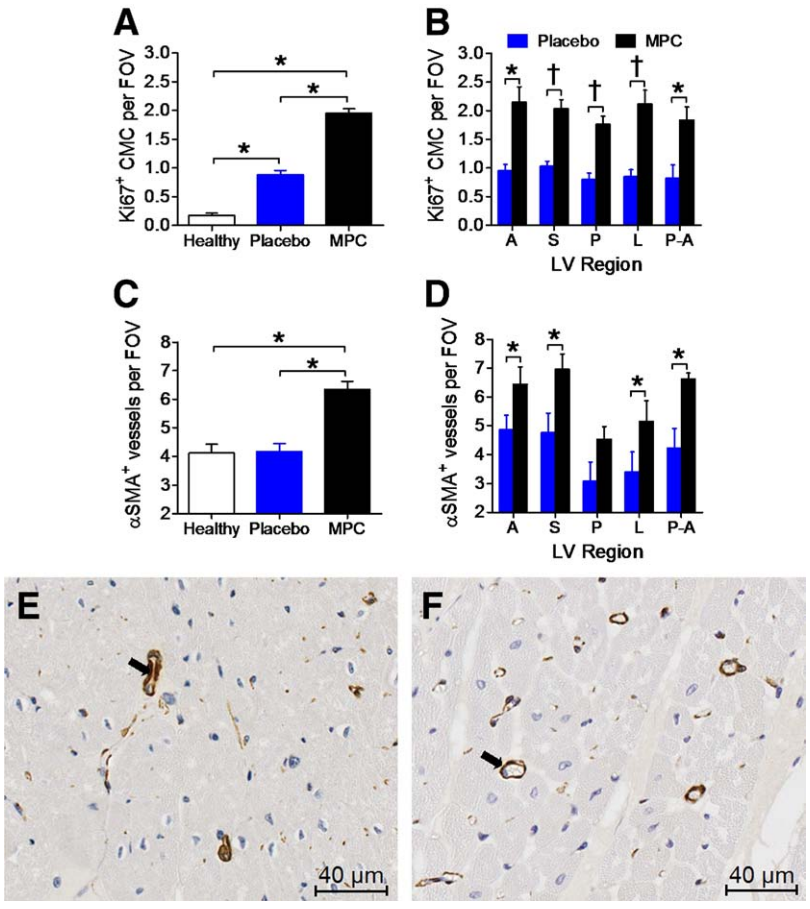

Figure 6. Effect of MPC on Cardiomyocyte Karyokinesis and Vascularity

The presence of cardiomyocytes in active cell cycle (Ki67$^+$) was augmented after MPC transplantation compared with placebo (1-way analysis of variance $p < 0.0001$) **(A)**, an effect that was observed throughout all myocardial walls (2-way analysis of variance $p < 0.0001$) **(B)**. Alpha-smooth muscle actin-positive blood vessels were also more prevalent after MPC treatment (1-way analysis of variance $p < 0.0001$) **(C)**. Despite segmental heterogeneity, MPC enhanced vascular density in the majority of left ventricular regions (2-way analysis of variance $p < 0.0001$) **(D)**. Representative examples of alpha–smooth muscle actin-positive staining **(arrows)** are shown from the placebo **(E)** and MPC groups **(F)**. *$p < 0.05$, †$p < 0.01$. αSMA$^+$ = alpha–smooth muscle actin-positive; FOV = field of view at ×20 magnification; Ki67$^+$ CMC = cardiomyocytes in active cell cycle; other abbreviations as in Figures 1 and 2.

the utility of the stromal precursor antigen-1, STRO-1, mAb has been well described for preparation of human MPC (14,15), its applicability has not extended to large animal species routinely used for cardiovascular research, due to its lack of reactivity with porcine or ovine MPC. In light of this, the STRO-3 mAb (16) was used in the present study to isolate clonogenic colony forming units-fibroblast with multilineage differentiation capacity and immunophenotypic characteristics of MSC. Rambouillet-derived MPC were administered to Merino sheep in order to simulate allogeneic transplantation. This may have special relevance clinically for patients in whom autologous BM cell therapy is compromised by either advanced age or chronic disease states, including cardiomyopathy (22).

Translational studies of MSC/MPC in NICM. Previous evaluation of MSC therapy in NICM has been restricted to small animal studies. In a rodent study of dilated cardiomyopathy, created by immunization with porcine cardiac myosin, transplantation of isogenic MSC resulted in improved LV function, enhanced capillary density, and reduced myocardial fibrosis (5). Mechanistic roles were implicated for both direct (regenerative transdifferentiation) and indirect (paracrine support) activity of engrafted cells. Similar benefits have been attributed to MSC in other small animal studies of toxic (7), metabolic (23), and infectious (6) cardiomyopathy. However, corresponding results in large animal or clinical studies have thus far been lacking. Therefore, in the present study, we evaluated MPC therapy in an ovine model of anthracycline-induced cardiomyopathy that consists of reproducible, moderate-severe LV dysfunction, with extensive cardiomyocyte, small-vessel and Purkinje fiber injury and increased myocardial fibrosis (19,21).

JACC: CARDIOVASCULAR INTERVENTIONS, VOL. 3, NO. 9, 2010
SEPTEMBER 2010:974–83

Transendocardial cell delivery. Although myocardial cell retention is suboptimal with all delivery routes thus far examined, studies suggest that superior results are obtained when cells are delivered by direct intramyocardial injection, compared with intracoronary or peripheral venous infusion (24,25). This is highly relevant in NICM, where the recruitment of exogenous cells across the myocardial vascular bed may be limited by a paucity of inflammatory, homing signals (26). Furthermore, the safety of intracoronary administration of MSC/MPC remains contentious as the physical properties of these cells may result in occlusion of the coronary microvasculature (24). For these reasons, we administered cells by direct, intramyocardial injection, adopting a catheter-based, transendocardial approach, due to it being less invasive and more clinically relevant than open, transepicardial injection. We used 3-dimensional electromechanical navigation to target unhealthy myocardium (21) and achieve multisegmental distribution of injections to enhance the prospects of achieving global LV repair.

Cell dose was selected on the basis of recent experience with MPC therapy in acute myocardial infarction, in which better outcomes were associated with 75×10^6 cells than higher doses (225×10^6 or 450×10^6 cells) (18). Placebo or cells were administered 10 weeks after first exposure to doxorubicin; by which stage, sheep had developed moderate LV dysfunction and evidence of electrical remodeling. Intraprocedural complications from intramyocardial injection were limited to 2 instances of supraventricular arrhythmia in the placebo cohort. However, all interventions were associated with elevations in serum troponin-T, indicating that early myocardial injury may have been caused by the injection process itself or by the cryopreservant agent that was common to both groups. Although the long-term consequences of injection site injury/inflammation are difficult to ascertain, the burden of fibrosis in placebo-injected animals was consistent with the level that we have previously noted in other doxorubicin NICM sheep (21).

Effects of MPC in experimental NICM. We observed higher attrition in the placebo group with surviving animals showing signs of deterioration that consisted of LV chamber expansion, progressive decline of systolic function, elevation of pulmonary capillary wedge pressure, reduction of arterial blood pressure, and prolongation of total electrical activation time. By comparison, MPC therapy was associated with attenuation of LV end-systolic dilation and contractile dysfunction and trends consistent with greater hemodynamic and electrical stability.

The relatively sparse presence of GFP-labeled MPC in the myocardium 4 weeks after injection suggests that these beneficial effects were unlikely to be due to direct substitution of lost cardiac cell mass. It is more conceivable that transient retention of MPC following their administration provided a paracrine stimulus for endogenous repair processes, thereby reducing fibrosis, stimulating neovascularization and cardiomyocyte karyokinesis. These histological outcomes were manifest globally in the LV, in line with the multisegmental approach used to deliver MPC.

Myocardial fibrosis has been shown to be an important contributor to the severity of systolic dysfunction and the development of adverse outcomes in NICM (27). Here, we showed that the burden of fibrosis was lower after MPC injection compared with placebo, although it was still greater than that measured in healthy heart specimens. This is consistent with the finding that cell therapy prevented progression of LV dysfunction, without reversing cardiac remodeling or restoring function to healthy baseline. The antifibrotic properties of MSC/MPC may be due to paracrine actions mediated by antifibrotic cytokines, such as hepatocyte growth factor (5,18,28). During in vitro experiments, we have found that STRO-3–selected MPC produce an array of cardiovascular-relevant factors, including hepatocyte growth factor, stromal cell-derived factor 1-alpha, and vascular endothelial growth factor that also mediate antiapoptotic, proangiogenic, and promitogenic responses (F. See, August 2010).

Even in the presence of angiographically normal coronary arteries, NICM has been associated with disturbances to myocardial blood flow (29). The increase in myocardial vascularity that we observed with MPC therapy may have assisted in limiting the progression of cardiomyopathy. In part, this may have been mediated by protecting the viability of cardiomyocytes, including those undergoing karyokinesis ($Ki67^+$). Although the precise nature of these $Ki67^+$ cells was not examined further, their increased presence following MPC transplantation could represent paracrine stimulation of mature cardiomyocytes or cardiac progenitor cells into active cycle.

Conclusions

This study investigated the unique combination of selectively prepared, allogeneic MPC administered by guided, multisegmental, transendocardial injections in a large animal model of NICM. The efficacy of this cell/delivery strategy manifested as attenuation of global systolic dysfunction, accompanied by pleiotropic effects on myocardial histology. Pending clinical studies, these results suggest that the reparative properties of MPC may extend their utility to the nonischemic context of cardiac disease.

Acknowledgments
The authors thank Dr. Tim Kuchel, Adrian Hines, Melissa Gourlay, Jodie Dier, Danijela Menicanin, Sharon Paton, and Sofie Kogoj (Institute of Medical and Veterinary Science/Hanson Institute) for their assistance during this study.

Reprint requests and correspondence: Dr. Peter J. Psaltis, Cardiovascular Investigation Unit, Royal Adelaide Hospital, North Terrace, Adelaide, South Australia 5000, Australia. E-mail: peter.psaltis@adelaide.edu.au.

REFERENCES

1. Felker GM, Thompson RE, Hare JM, et al. Underlying causes and long-term survival in patients with initially unexplained cardiomyopathy. N Engl J Med 2000;342:1077–84.
2. Gersh BJ, Simari RD, Behfar A, Terzic CM, Terzic A. Cardiac cell repair therapy: a clinical perspective. Mayo Clin Proc 2009;84:876–92.
3. Seth S, Narang R, Bhargava B, et al., on behalf of AIIMS Cardiovascular Stem Cell Study Group. Percutaneous intracoronary cellular cardiomyoplasty for nonischemic cardiomyopathy: clinical and histopathological results: the first-in-man ABCD (Autologous Bone Marrow Cells in Dilated Cardiomyopathy) trial. J Am Coll Cardiol 2006;48:2350–1.
4. Fischer-Rasokat U, Assmus B, Seeger FH, et al. A pilot trial to assess potential effects of selective intracoronary bone marrow-derived progenitor cell infusion in patients with nonischemic dilated cardiomyopathy: final 1-year results of the transplantation of progenitor cells and functional regeneration enhancement pilot trial in patients with nonischemic dilated cardiomyopathy. Circ Heart Fail 2009;2:417–23.
5. Nagaya N, Kangawa K, Itoh T, et al. Transplantation of mesenchymal stem cells improves cardiac function in a rat model of dilated cardiomyopathy. Circulation 2005;112:1128–35.
6. Guarita-Souza LC, Carvalho KA, Woitowicz V, et al. Simultaneous autologous transplantation of cocultured mesenchymal stem cells and skeletal myoblasts improves ventricular function in a murine model of Chagas disease. Circulation 2006;114:I120–4.
7. Garbade J, Dhein S, Lipinski C, et al. Bone marrow-derived stem cells attenuate impaired contractility and enhance capillary density in a rabbit model of doxorubicin-induced failing hearts. J Card Surg 2009;24:591–9.
8. Psaltis PJ, Zannettino AC, Worthley SG, Gronthos S. Concise review: mesenchymal stromal cells: potential for cardiovascular repair. Stem Cells 2008;26:2201–10.
9. Silva GV, Litovsky S, Assad JA, et al. Mesenchymal stem cells differentiate into an endothelial phenotype, enhance vascular density, and improve heart function in a canine chronic ischemia model. Circulation 2005;111:150–6.
10. Amado LC, Saliaris AP, Schuleri KH, et al. Cardiac repair with intramyocardial injection of allogeneic mesenchymal stem cells after myocardial infarction. Proc Natl Acad Sci U S A 2005;102:11474–9.
11. Quevedo HC, Hatzistergos KE, Oskouei BN, et al. Allogeneic mesenchymal stem cells restore cardiac function in chronic ischemic cardiomyopathy via trilineage differentiating capacity. Proc Natl Acad Sci U S A 2009;106:14022–7.
12. Hare JM, Traverse JH, Henry TD, et al. A randomized, double-blind, placebo-controlled, dose-escalation study of intravenous adult human mesenchymal stem cells (prochymal) after acute myocardial infarction. J Am Coll Cardiol 2009;54:2277–86.
13. Pittenger MF, Martin BJ. Mesenchymal stem cells and their potential as cardiac therapeutics. Circ Res 2004;95:9–20.
14. Psaltis PJ, Paton S, See F, et al. Enrichment for STRO-1 expression enhances the cardiovascular paracrine activity of human bone marrow-derived mesenchymal cell populations. J Cell Physiol 2010; 223:530–40.
15. Gronthos S, Zannettino AC, Hay SJ, et al. Molecular and cellular characterisation of highly purified stromal stem cells derived from human bone marrow. J Cell Sci 2003;116:1827–35.
16. Gronthos S, Fitter S, Diamond P, Simmons PJ, Itescu S, Zannettino AC. A novel monoclonal antibody (STRO-3) identifies an isoform of tissue nonspecific alkaline phosphatase expressed by multipotent bone marrow stromal stem cells. Stem Cells Dev 2007;16:953–63.
17. Martens TP, See F, Schuster MD, et al. Mesenchymal lineage precursor cells induce vascular network formation in ischemic myocardium. Nat Clin Pract Cardiovasc Med 2006;3 Suppl 1:S18–22.
18. Dixon JA, Gorman RC, Stroud RE, et al. Mesenchymal cell transplantation and myocardial remodeling after myocardial infarction. Circulation 2009;120:S220–9.
19. Psaltis PJ, Carbone A, Nelson A, et al. An ovine model of toxic, nonischemic cardiomyopathy—assessment by cardiac magnetic resonance imaging. J Card Fail 2008;14:785–95.
20. Psaltis PJ, Worthley SG. Endoventricular electromechanical mapping—the diagnostic and therapeutic utility of the NOGA® XP Cardiac Navigation System. J Cardiovasc Transl Res 2009;2:48–62.
21. Psaltis PJ, Carbone A, Leong DP, et al. Assessment of myocardial fibrosis by endoventricular electromechanical mapping in experimental nonischemic cardiomyopathy. Int J Cardiovasc Imaging 2010 Jun 29 [E-pub ahead of print].
22. Kissel CK, Lehmann R, Assmus B, et al. Selective functional exhaustion of hematopoietic progenitor cells in the bone marrow of patients with postinfarction heart failure. J Am Coll Cardiol 2007;49:2341–9.
23. Zhang N, Li J, Luo R, Jiang J, Wang JA. Bone marrow mesenchymal stem cells induce angiogenesis and attenuate the remodeling of diabetic cardiomyopathy. Exp Clin Endocrinol Diabetes 2008;116:104–11.
24. Freyman T, Polin G, Osman H, et al. A quantitative, randomized study evaluating three methods of mesenchymal stem cell delivery following myocardial infarction. Eur Heart J 2006;27:1114–22.
25. Perin EC, Silva GV, Assad JA, et al. Comparison of intracoronary and transendocardial delivery of allogeneic mesenchymal cells in a canine model of acute myocardial infarction. J Mol Cell Cardiol 2008;44:486–95.
26. Theiss HD, David R, Engelmann MG, et al. Circulation of CD34+ progenitor cell populations in patients with idiopathic dilated and ischaemic cardiomyopathy (DCM and ICM). Eur Heart J 2007;28: 1258–64.
27. Assomull RG, Prasad SK, Lyne J, et al. Cardiovascular magnetic resonance, fibrosis, and prognosis in dilated cardiomyopathy. J Am Coll Cardiol 2006;48:1977–85.
28. Gnecchi M, Zhang Z, Ni A, Dzau VJ. Paracrine mechanisms in adult stem cell signaling and therapy. Circ Res 2008;103:1204–19.
29. Parodi O, De Maria R, Oltrona L, et al. Myocardial blood flow distribution in patients with ischemic heart disease or dilated cardiomyopathy undergoing heart transplantation. Circulation 1993;88:509–22.

Key Words: cell therapy ■ electromechanical mapping ■ mesenchymal precursor cells ■ mesenchymal stem cells ■ nonischemic cardiomyopathy.

APPENDIX

For expanded description of the methods, please see the online version of this article.